Hindawi
Stem Cells International
Volume 2022, Article ID 6593403, 13 pages
https://doi.org/10.1155/2022/6593403

Research Article

Optimizing the Method for Differentiation of Macrophages from Human Induced Pluripotent Stem Cells

Shanshan Li,[1] Lili Song,[2] Yingwen Zhang,[1] Zhiyan Zhan,[1] Yi Yang,[1] Lisha Yu,[2] Hua Zhu,[2] Weihua Huang,[3] Wanqiao Wang,[1] Haizhong Feng,[4] and Yanxin Li[1]

[1]*Pediatric Translational Medicine Institute, Shanghai Children's Medical Center, School of Medicine, Shanghai Jiao Tong University, National Health Committee Key Laboratory of Pediatric Hematology & Oncology, Shanghai 200127, China*
[2]*Department of Hematology & Oncology, Shanghai Children's Medical Center, School of Medicine, Shanghai Jiao Tong University, National Health Committee Key Laboratory of Pediatric Hematology & Oncology, Shanghai 200127, China*
[3]*Department of Transfusion Medicine, The First Affiliated Hospital of Naval Medical University, Shanghai 200433, China*
[4]*State Key Laboratory of Oncogenes and Related Genes, Renji-Med X Clinical Stem Cell Research Center, Renji Hospital, Shanghai Cancer Institute, Shanghai Jiao Tong University School of Medicine, Shanghai 200127, China*

Correspondence should be addressed to Haizhong Feng; fenghaizhong@sjtu.edu.cn and Yanxin Li; 18930837583@163.com

Received 6 August 2021; Revised 21 January 2022; Accepted 4 February 2022; Published 3 March 2022

Academic Editor: Federico Mussano

Macrophage is a very promising cell type for cancer immunotherapy, yet it is difficult to obtain enough functional macrophages for clinical cell therapy. Herein, we descibe a reliable method to produce functional macrophages through the differentiation of human induced pluripotent stem cells (hiPSCs). By optimizing the size control of embryoid bodies (EBs), we accelerated the differentiation process of macrophages and increased the production of macrophages without attenuating macrophage functions. Our final yield of macrophages was close to 50-fold of starting iPSCs. The macrophages showed phagocytic capacity in vitro and a xenograft tumor model. M0 macrophages could be further polarized into M1 and M2 subtypes, and M1 cells exhibited typical proinflammatory characteristics. Moreover, we found that hematopoietic differentiation originated from the outside of EB and matured inward gradually. Taken together, our protocol provides an effective method for the generation of macrophages comparable to blood-derived macrophages, which provides potential value for cell therapy and gene editing studies.

1. Introduction

Adoptive cell therapy, such as chimeric antigen receptor (CAR) T cell therapy, provides a revolutionary approach for cancer therapy, but its application in solid tumors still has some limitations [1]. Macrophages, the most plastic type of white blood cells of the immune system, play important roles in development, homeostasis, and cancer [2]. Since they can immerse in the tumor environment, enhance the cytotoxic effects of T cells, and have less no-tumor toxicity, CAR-macrophage has shown more advantages in the treatment of solid tumors [3]. However, due to the characteristic of terminal differentiation of macrophages [4], it is hard to obtain adequate amounts of cells.

The most common sources of human macrophages include peripheral blood or bone marrow monocytes, myeloid cell lines (such as THP-1), and pluripotent stem cells. Nevertheless, isolation of monocytes is time-consuming and the yield is low, and the myeloid cell lines cannot replicate the complexity of macrophages in vivo [5]. Macrophages derived from human embryonic stem cells have the same functions as macrophages from peripheral blood and bone marrow monocytes, but there

are ethical issues involved [5]. hiPSCs become a favorable choice, because they have no ethical limitations and can be easily manipulated by genome editing technology [6–9].

In the past few years, the differentiation schemes of iPSC-derived macrophages (IPSDMs) have been constantly inproved and used in disease models [10–15], macrophage-pathogen interaction modeling [16, 17], and cell therapy [18]. Initially, cells in some methods were required to coculture with OP9 mouse stromal cells [10, 19, 20], but this approach was gradually obsoleted because of the use of xenogeneic cells that limited the clinical application. At present, hiPSC differentiation schemes are mainly based on the form of EB or monolayer cultivation (Table S1). Compared with monolayer cultivation protocols, EB protocols have the advantage of allowing a continuous harvest of suspension cells for the long-term production of macrophages with relatively few cytokines [21–26]. By contrast, monolayer cultivation protocols achieved higher one-off collection rates of macrophage by modified differentiation steps, such as a complex mixture of factors [27–30] (up to 11 factors), hypoxia conditions [28], and CD14 sorting [29, 30]. In the past, the seeding number of iPSCs per EB in most EB-based protocols was unfixed. The size of EB was random and the yield was not stable [22–25, 31, 32]. Continuous generation of IPSDMs resulted in high cumulative yield, but the efficiency of amplification was not high enough to obtain sufficient quantities of macrophages in a short time [21, 22, 25]. Thus, it is necessary to establish a convenient and less expensive differentiation scheme that can achieve higher yields in the short term.

In this study, by optimizing EB size, we accelerated the differentiation process of macrophages and increased the production of macrophages without attenuating macrophage functions.

2. Material and Methods

2.1. hiPSC Culture. hiPSCs were cultured in feeder-free, serum-free PSCeasy® II medium (Cellapy) and were passaged when the cells reached 70%-80% confluency. To passage cells, the medium was aspirated and 1 ml 0.5 mM EDTA (Invitrogen) was added to each well of one 6-well plate, and then, cells were incubated for 4-5 min at 37°C. Each well of one 6-well plate could be transferred to one 6-well plate by 1 : 6 split ratio. 2 ml medium per well was dispensed to Matrigel (BD Biosciences)-coated 6-well plates, and the plate was returned to an incubator at 37°C, 5% CO_2.

2.2. Differentiation of hiPSCs into Macrophages. We performed hematopoietic differentiation of hiPSCs by using two versions of the EB-based hematopoietic differentiation protocol. First, hiPSC colonies were incubated with 1 ml TrypLE Express (Gibco) for 2 min at room temperature. In the P3500 protocol, the TrypLE Express was aspirated, and the cells were resuspended with APEL (STEMCELL Technologies) and disrupted to a single cell suspension by pipetting up and down, supplemented with 10 μM Rock inhibitor Y27632 (STEMCELL Technologies), 10 ng/ml BMP4 (R&D Systems), and 10 ng/ml recombinant human bFGF (R&D Systems). Cells (3500/well) were seeded into 60 wells in the middle of an untreated round-bottom 96-well plate (Costar 3788) and centrifuged at 300 × g at room temperature for 5 min. From day 2 to day 14, the cells were cultured in APEL containing BMP4 (10 ng/ml), bFGF (10 ng/ml), VEGF (PeproTech) (10 ng/ml), and SCF (PeproTech) (50 ng/ml). On day 14, the APEL medium was removed, and then, macrophage differentiation medium RPMI Medium 1640 basic (Gibco) was added, supplemented with 10% fetal bovine serum (FBS, Gibco), 1% penicillin-streptomycin (PS, NCMBIO), 100 ng/ml M-CSF (PeproTech), and 25 ng/ml IL-3 (PeproTech). On day 22, both EBs and single cells in suspension were harvested and then filtered through 100 μm cell strainers to remove the EBs. The cells were centrifuged at 1000 rpm for 5 min and seeded into the 6-well tissue culture plate. After day 22, aspirate the spent medium and add fresh macrophage differentiation medium (RPMI 1640+10% FBS+1% PS+100 ng/ml M-CSF) as needed if the medium turned yellow.

In the P8000 protocol, the cells were resuspended with APEL supplemented with 10 μM Rock inhibitor Y27632, 10 ng/ml recombinant human bFGF, 20 ng/ml BMP4, 20 ng/ml VEGF, and 40 ng/ml SCF. Cells (8000/well) were seeded into 60 wells in the middle of nontreated round-bottom 96-well plates in 100 μl medium per well. From day 0 to day 8, 100 μl APEL medium was removed and the above medium (no Y27632) was added every 2~3 days. On day 8, aspirate APEL medium and replace with fresh macrophage differentiation medium (RPMI1640+10% FBS+1% PS+100 ng/ml M-CSF+25 ng/ml IL-3). On day 14, the EBs and cells were collected and seeded into round-bottom 6-well plates (Costar 3471), and suspension cells were harvested in the supernatants. The EBs were removed until day 22. The rest was as described in the P3500 protocol.

2.3. Flow Cytometry Analysis. Cells were washed once and stained with antibodies or isotype control for 30 minutes at 4°C in flow cytometry buffer. The samples were analyzed on FACS Calibur (BD Canto Plus), and data were analyzed using FlowJo v10 (FlowJo, LLC). The following antibodies were used: CD45-APC-Cy7 (2D1, IgG1κ-APC-Cy7) from BioLegend; CD34-PE (4H11, IgG1κ-PE) and CD14-PE (61D3, IgG1κ-PE) from Invitrogen; CD11b-APC (M1/70, IgG2bκ-APC), CD80-PE (2D10.4, IgG1κ-PE), CD86-PE-Cy7 (IT2.2, IgG2bκ-PE-Cy7), CD163-PE (GHI/61, IgG1κ-PE), and CD206-PE-Cy7 (19.2, IgG1κ- PE-Cy7) from eBioscience.

2.4. Wright-Giemsa Staining. Cells were centrifuged at 500 rpm for 5 minutes and immobilized on microscope slides using cytospins (Tharmac Cellspin) followed by staining with Wright-Giemsa stain.

2.5. $CD14^+$ Monocyte Isolation. Peripheral blood mononuclear cells (PBMCs) were isolated from healthy donor blood by Ficoll-Paque (Cytiva), and $CD14^+$ monocytes were isolated from PBMCs using human CD14 Microbeads (Miltenyi Biotec) according to the manufacturer's instructions.

2.6. Differentiation of Macrophage Subtypes. The cells were differentiated into M0 cells at day 25 to day 30. M0 cells were polarized for 48 h to M1 cells in macrophage differentiation

medium supplemented with 100 ng/ml LPS (Sigma) and 20 ng/ml IFN-γ (PeproTech), to M2 cells in macrophage differentiation medium supplemented with 20 ng/ml IL-4 (PeproTech). Cells were detached using Accutase (Gibco) or 5 mM EDTA for 5-10 minutes.

2.7. Fluorescent Bead Phagocytosis Assay. Fluoresbrite™ Polychromatic Red 1.0 μm Latex beads (Polyscience Inc., 18660) were added to the cell culture medium. After 24 hours, macrophages were washed and analyzed by confocal microscopy or flow cytometry.

2.8. Tumor Phagocytosis Assay. Reh and Nalm6 tumor cells were stained with Hoechst 33342 (Life Technologies) at 37°C for 20 minutes. Then, the cells were washed with PBS three times and 1×10^5 macrophages were cocultured with tumor cells in the proportions of 1 : 1, 1 : 2, or 1 : 4, respectively, and then incubated for 2 hours at 37°C. Cells were seeded into a round-bottom 96-well plate at a density of 1×10^5/well in 200 μl macrophage medium. The cells were harvested and stained with CD11b-APC antibody at 4°C for 30 minutes, and then, the phagocytosis ratio was measured by FACS Calibur. Macrophages were cocultured with tumor cells in the proportions of 1 : 4 in M0, M1, and M2 phagocytosis assay.

2.9. Immunofluorescence. First, cells were fixed in 4% paraformaldehyde (PFA) for 20 minutes and then washed three times using PBS. For bead phagocytosis assay, the cells were stained with 5 μg/ml Wheat Germ Agglutinin (WGA), Alexa Fluor 633 Conjugates (Invitrogen) for 10 minutes and then washed twice using PBS followed by DAPI (1 : 500) staining as standard procedures. Undifferentiated hiPSCs were used as control. For the tumor phagocytosis assay, the cocultured cells were blocked with 10% goat serum and then incubated with CD11b-APC antibody at 4°C overnight; then, the antibody was washed away. The images were captured by a confocal laser scanning microscope (Leica SP8).

2.10. Frozen Section and Immunofluorescence of EBs. EBs were collected and embedded using optimal cutting temperature compound followed by frozen section, and the microscope slides were stored at -80°C. For immunofluorescence, microscope slides were left at room temperature for 15 minutes and immersed in PBS for 10 minutes to remove OCT. Then, EBs were blocked with 10% goat serum and incubated with CD34-PE and CD45-APC-Cy7 antibody (1 : 100) at 4°C overnight, and then, the cells were washed and stained with DAPI as described above.

2.11. Cytokine Detection. M0 macrophages were cultured in macrophage differentiation medium until reaching more than 90% confluency. Then, M0 cells were polarized toward M1 and M2 cells with previously mentioned cytokines. Cell supernatants were collected and the concentration of cytokines was detected by AimPlex® multiplex immunoassays for Flow™ (QuantoBio).

2.12. Animal Study. All mouse studies were conducted in accordance with national guidelines for the humane treatment of animals and were approved by the Institutional Animal Care and Use Committee (IACUC) at Shanghai Jiao Tong University. CB17-SCID mice were divided into three groups, and cells were resuspended in 100 μl matrix and subcutaneously inoculated into the mice as (a) 2×10^6 Raji cells each mouse, (b) 2×10^6 Raji cells plus 7×10^6 PBDMs each mouse, and (c) 2×10^6 Raji cells plus 7×10^6 IPSDMs each mouse. Tumor formation was observed closely, and tumor volume was measured every 2-3 days when the tumors were visible. When the tumor grew to a certain size, the mice were sacrificed and tumors were dissected, photographed, and weighed. Tumor tissue was embedded in paraffin blocks for sectioning and staining with hematoxylin and eosin.

2.13. Statistical Analysis. All experiments were repeated three times or more. Two-tailed Student's unpaired *t*-test was used for pairwise statistical analysis, and multiple groups were evaluated by one-way ANOVA or two-way ANOVA followed by Bonferroni's multiple comparisons test. Data are presented as the mean ± SD. $P < 0.05$ was considered statistically significant.

3. Results

3.1. The Quantity of Seeding Cells Affected the Process of hiPSCs Differentiated into Macrophages. Macrophage differentiation from iPSCs needs three steps: hematopoietic differentiation, expansion of myeloid progenitors, and maturation of macrophages. Here, we used two protocols, P3500 and P8000, to compare macrophage differentiation efficacy from hiPSCs (Figure 1(a)). In the P3500 protocol, hiPSCs (3500/well) were seeded in an untreated round-bottom 96-well plate and the culture medium was replaced with macrophage differentiation medium on day 14. In the P8000 protocol, hiPSCs (8000/well) were seeded and the culture medium was replaced on day 8. The percentage of $CD34^+CD45^+$ cells was more than 80% on day 14 in the P3500 protocol (Figure 1(d), Figure S1a), but the rate of $CD34^+CD45^+$ cells was no more than 20% and the $CD45^+CD14^+$/$CD45^+CD11b^+$ cells have reached 40%~60% at day 14 in the P8000 protocol (Figures 1(c) and 1(d), Figure S1a). Myeloid cells could be harvested from the EB culture supernatant in the P8000 protocol at day 14, which was earlier than that in the P3500 protocol (Figures 1(b)–1(d)). From day 14 to day 22, $CD34^+CD45^+$ hematopoietic progenitor cells (HPCs) were differentiated into myeloid progenitor cells in the P3500 protocol. On day 22, the percentage of $CD45^+CD14^+$/$CD45^+CD11b^+$ cells reached about 70% in the P3500 protocol, while that positive rate of P8000 protocol was higher (Figures 1(c) and 1(d), Figure S1b). At the end of the second step, cells can be frozen or differentiated into a more mature state. On day 30, there were no differences in the percentage of $CD45^+CD14^+$/$CD45^+CD11b^+$ cells between the two protocols (Figures 1(c) and 1(d), Figure S1c). Overall, the differentiation process of macrophages in the P8000 protocol was faster than that in the P3500 protocol. More importantly, the number of total cells harvested in the P8000 protocol was higher than that of the P3500 protocol on day 22 and day 30 (Figure 1(e)). At last, about $(1 \sim 2) \times 10^7$ cells were collected per 96-well plate in the P8000 protocol at day 30. During the differentiation

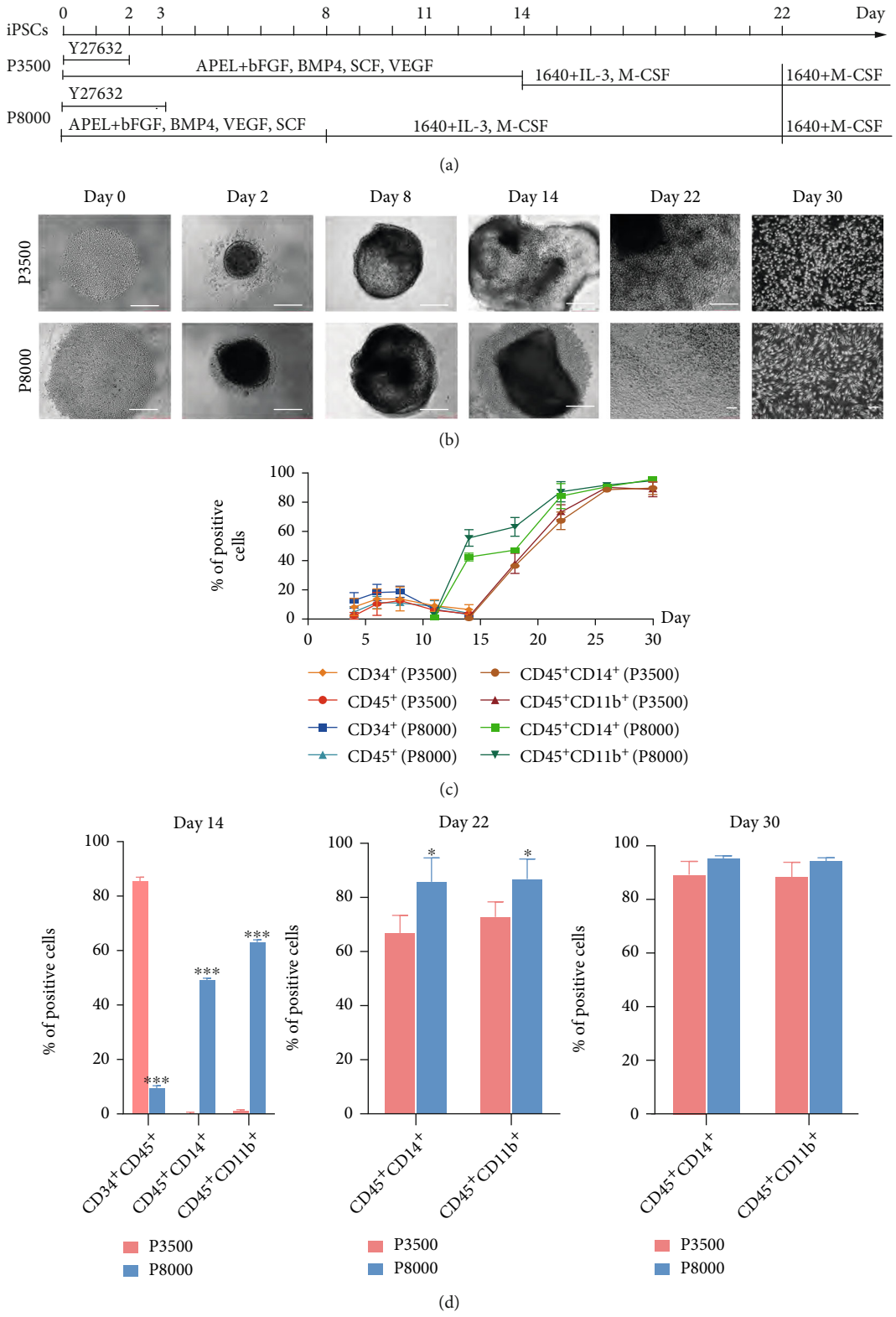

Figure 1: Continued.

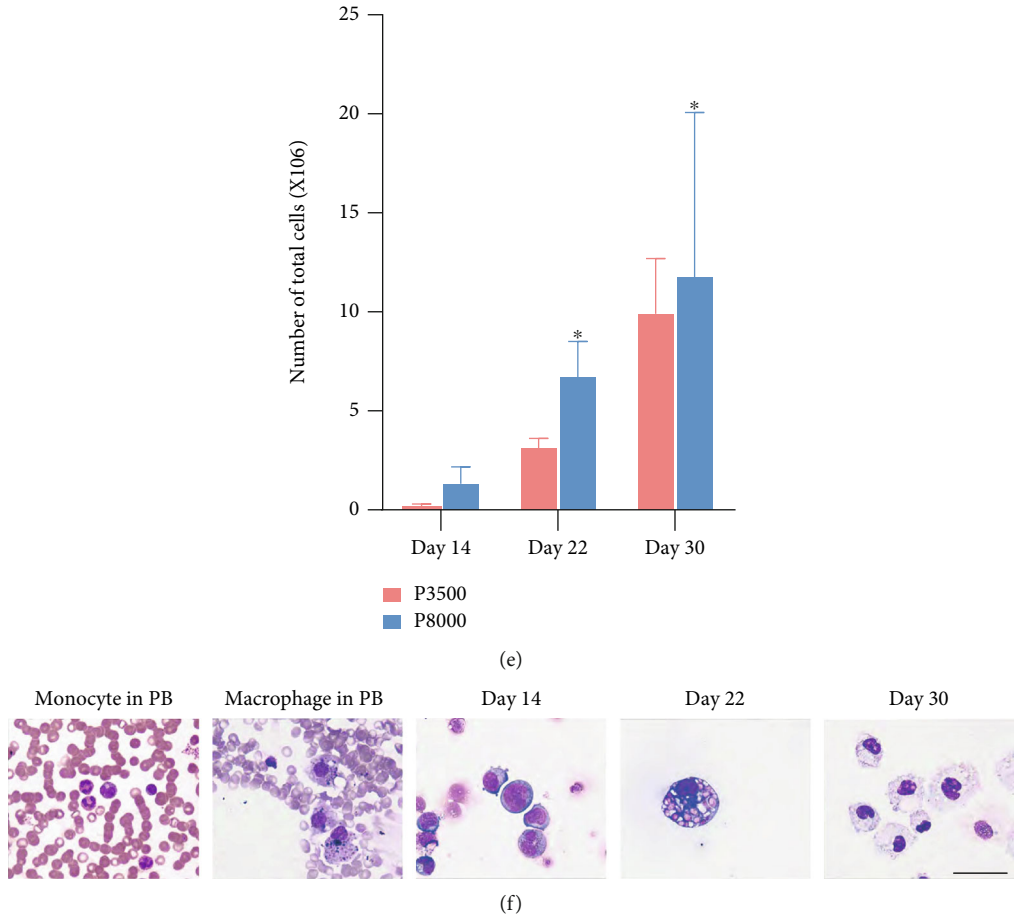

Figure 1: The quantity of seeding cells affected the process of hiPSCs differentiated into macrophages. (a) Schematic diagram of the protocols of macrophage differentiation from hiPSCs. (b) Representative bright-field images of EBs and cells at different time points during culture stages under two macrophage differentiation protocols. Scale bars, 250 μm. (c) The percentages of different cell types ($CD34^+$, $CD45^+$, $CD45^+CD14^+$, and $CD45^+CD11b^+$) produced during the different culture stages under two macrophage differentiation protocols. (d) The percentage of $CD34^+CD45^+$ cells at day 14 and $CD45^+CD14^+/CD45^+CD11b^+$ cells at day 14, day 22, and day 30 in two macrophage differentiation protocols. $^*P < 0.05$ and $^{***}P < 0.001$. (e) The total number of cells at day 14, day 22, and day 30 in two macrophage differentiation protocols. $^*P < 0.05$. (f) Representative Wright-Giemsa staining images of monocytes and macrophages in peripheral blood and cells differentiated from hiPSCs at day 14, day 22, and day 30 in the P3500 protocol. Scale bar represents 50 μm.

process of the P3500 protocol, the cells of day 14, day 22, and day 30 were stained by Wright-Giemsa stain (Figure 1(f)). On day 14, there were mainly immature hematopoietic cells. On day 22, the monocyte showed typical morphological characteristics and had more vacuoles in the cytoplasm than that of monocytes in peripheral blood. On day 30, the cells were more mature, like "fried eggs." These results suggested that the quantity of seeding cells and time to add cytokines determined the differentiation efficiency.

3.2. More Seeding Cells Promoted the Development of HPCs in EBs. To further explore the development of HPCs in EBs, EBs of the two protocols at different time points were observed by freezing section and immunofluorescence staining. On day 4, $CD34^+$ and $CD45^+$ cells could be observed in the P8000 protocol, but hardly in the P3500 protocol by immunofluorescence (Figure 2(a)). On day 6, $CD34^+$ and $CD45^+$ cells were first found in the P3500 protocol by immunofluorescence (Figure 2(b)). In addition, we found that CD34 protein was mainly located in the outer layer of EBs which directly interacted with cytokines and gradually decreased as it went inward, while CD45 was mainly expressed in the inner layer of EBs which was going weaker outward (Figures 2(a)–2(c)). These results verified that HPCs were differentiated from EB outer layer to internal sac and the bigger EB promoted HPC differentiation.

3.3. The hiPSC-Derived Macrophages Possess the Function of Phagocytosis. Peripheral blood-derived macrophages (PBDMs) can phagocytose foreign substances, so we wanted to see if macrophages derived from hiPSCs also have phagocytic function. Firstly, we used the fluorescent beads to determine the phagocytic function of macrophages as previously described [28]. After macrophages were incubated with fluorescent beads for 24 hours, the macrophages were observed with laser confocal microscopy. To exclude a small number of fluorescence beads

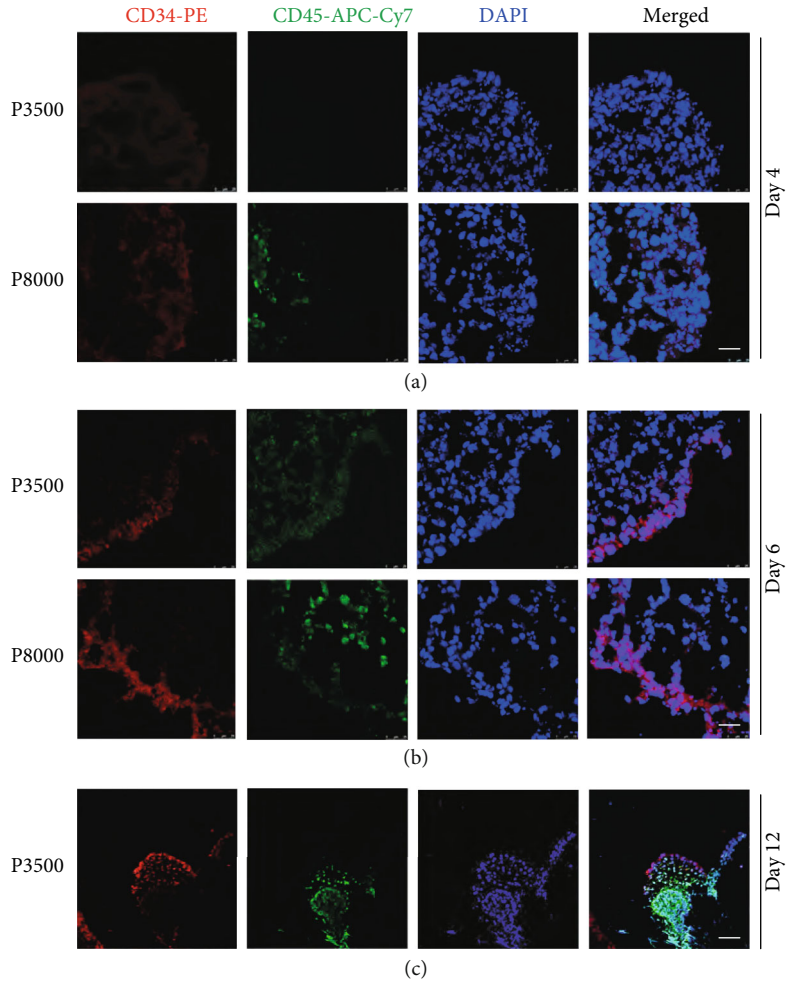

Figure 2: More seeding cells promoted the development of HPCs in EBs. (a–c) Frozen sections and immunofluorescence images of EBs in two macrophage differentiation protocols. Immunocytochemical analysis of CD34 (red) and CD45 (green) at day 4, day 6, and day 12. DAPI (blue) shows the cell nuclei (scale bars: 25 μm in (a) and (b), 50 μm in (c)).

still stuck to the cells causing false positives, we used hiPSCs as a control. Obviously, the fluorescent beads were located inside the macrophages, while the fluorescent beads were scattered on the surface in the hiPSCs group (Figure 3(c)). Flow cytometry also confirmed the phagocytosis of fluorescent beads by macrophages, and there was no difference in the phagocytosis of macrophages between the two differentiation protocols (Figures 3(a) and 3(b)).

Next, we further verified the phagocytosis ability of macrophages toward tumor cells. First, leukemia cell lines, Nalm6 and Reh, were labeled with Hoechst 33342 fluorochrome, and then, macrophages and tumor cells were coincubated. When the ratio of macrophages to tumor cells was 1 : 4, the proportion of macrophages that had phagocytosed tumor cells was the highest, which was above 40%-50% (Figures 3(d) and 3(f)). We hypothesized that increased contact between tumor cells and macrophages promoted the phagocytosis of macrophages. The phagocytosis of macrophages on tumor cells was also captured by laser confocal microscopy (Figure 3(e)). The dynamic process of phagocytosis was recorded by real-time fluorescence imaging of living cells (Supplementary Data, Movie).

To determine whether differentiated macrophages also have antitumor activity in vivo, Raji cells with or without PBDMs or IPSDMs were subcutaneously inoculated into CB17-SCID mice. After more than one month of observation, there were no significant differences in the tumor weight and size among the three groups (Figures S2a and S2b). However, in the group treated with PBDMs or IPSDMs, dissolution and cavities were found inside the tumor tissues (Figure S2c). These results suggested that although our IPSDMs did not show an obvious antitumor effect in vivo, the function of IPSDMs in our protocol was comparable to that of PBDMs.

3.4. Identification of the Different Polarization Subtypes from IPSDMs. Macrophages are usually divided into two different activated states, namely, M1 (or classical activated) type, and M2 (or alternately activated) type. M1 phenotype is proinflammatory which has strong antimicrobial and antitumor activity, while M2 is considered to promote tissue remodeling and tumor growth [33]. Under continuous induction of M-CSF, the myeloid progenitor cells adhered to the six-well plate and were differentiated into M0 macrophages. M0 cells could be polarized toward M1 cells by LPS and

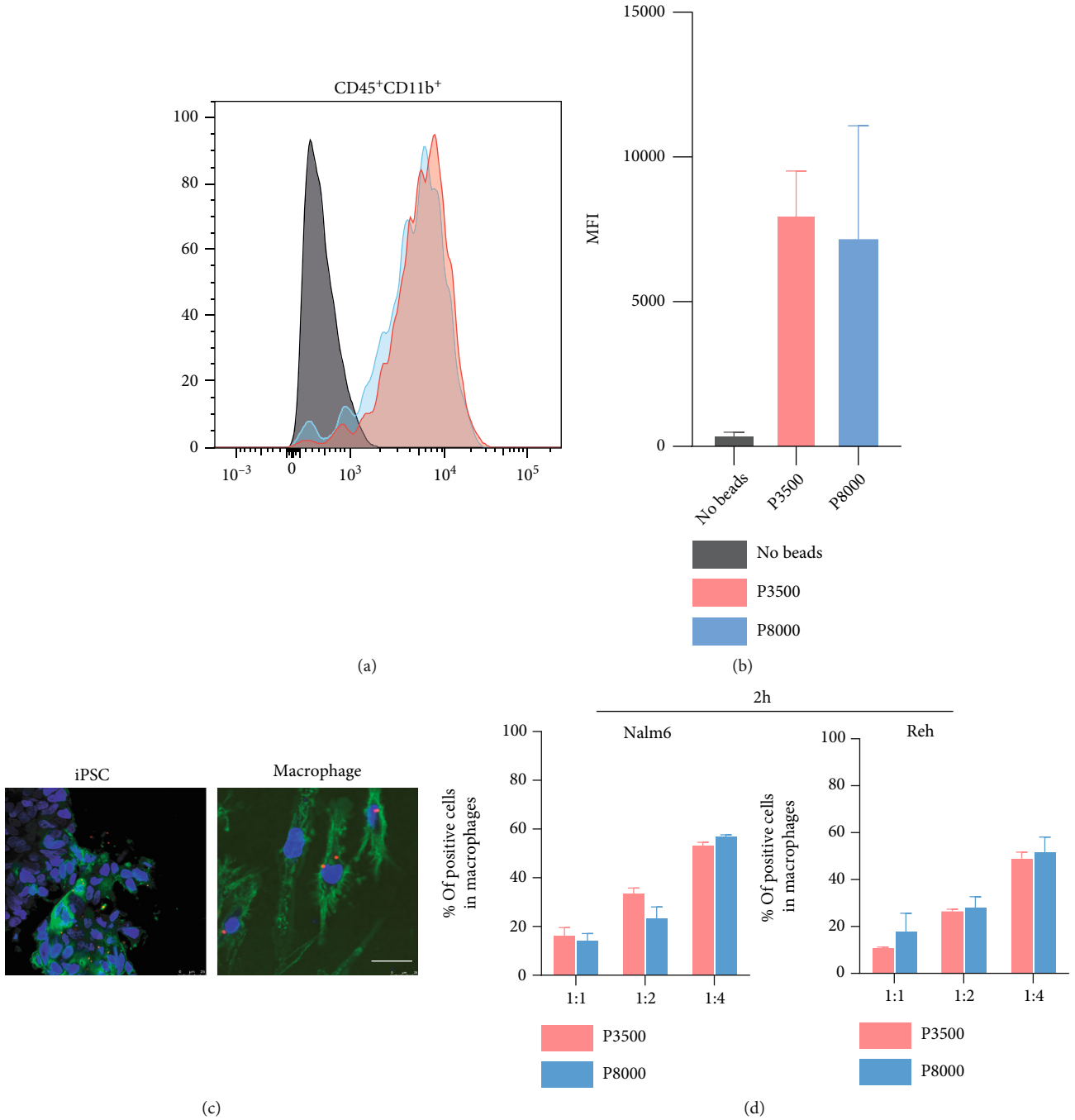

Figure 3: Continued.

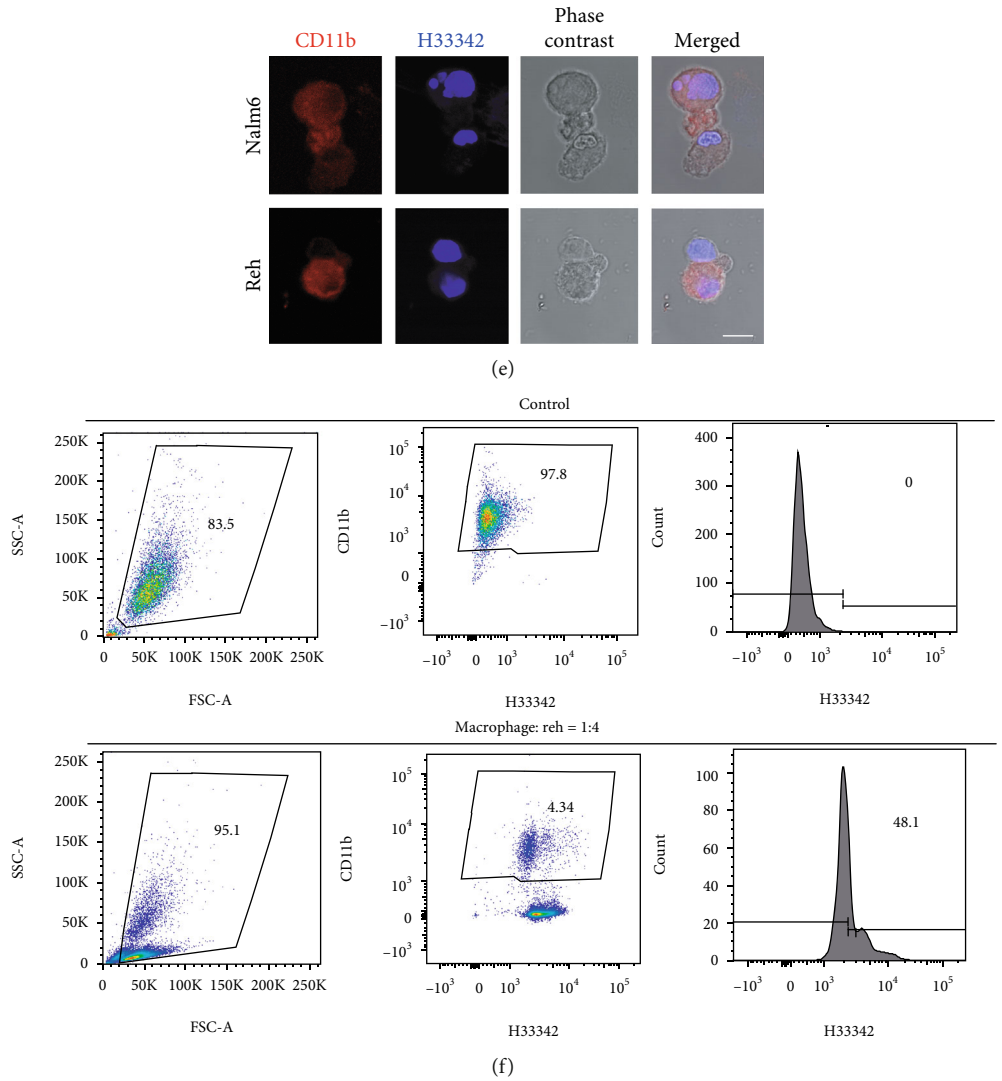

Figure 3: The hiPSC-derived macrophages possess the function of phagocytosis. (a, b) Flow cytometric analysis of the uptake of fluorescent beads by IPSDMs in two differentiation protocols. (c) Phagocytosis of fluorescent beads (red) by IPSDMs and IPSCs control. DAPI (blue) shows the cell nuclei; WGA (green) shows the cell membrane. Scale bars, 50 μm. (d) When the ratio of IPSDMs to tumor cells is 1 : 1, 1 : 2, or 1 : 4, the proportion of IPSDMs that have engulfed tumor cells is calculated. All experiments were performed three times. Error bars, SD. (e) Representative images of Nalm6 and Reh cells (labeled with Hoechst 33342) phagocytized by IPSDMs (labeled with CD11b and phase contrast image). Scale bars, 25 μm. (f) Flow cytometric analysis of phagocytosis of IPSDMs on Reh (IPSDM : Reh = 1 : 4). $CD11b^+$ macrophages are gated (middle panel), and V450 intensity is shown as a histogram (right panel). Macrophages cocultured with Reh-Hoechst 33342 suspension (after washing) as a negative control.

IFN-γ. Using IL-4, M0 cells could be polarized toward M2 cells. M0 cells were elongated in shape, M1 had more protrusions, and M2 cells were more rounded (Figure 4(a)), as previously described [29]. The expression of CD80 and CD86 was upregulated in M1 cells, and the expression of CD163 and CD206 was higher in M0 and M2 cells (Figure 4(b)). PBDMs and IPSDMs obtained similar results. Furthermore, the minor difference between IPS-M0 and IPS-M2 cells showed that the phenotype of M-CSF-induced macrophages had shifted toward M2 cells, as discussed by Zhang et al. [31]. Then, we investigated whether the phagocytic capacity of macrophages in different activated states differed. The results demonstrated that there was no difference in the phagocytic capacity between M0 and M2 cells, while that of M1 cells slightly decreased but had no statistical significance (Figures 4(c)–4(e)). And more, the phagocytic activity of IPSDMs was comparable to that of PBDMs (Figures 4(d) and 4(e)). Cytokine secretion showed that significantly higher levels of proinflammatory cytokines (IL-6 and TNF-α) were secreted in PB-M1 and IPS-M1 cells (Figure 4(f)). The results confirmed that macrophages from iPSCs could be polarized into different subtypes as macrophages derived from PB.

4. Discussion

In this study, we show an optimized differentiation method of IPSDMs to produce mature macrophages in a relatively short time with a higher yield. Macrophages have always been a hot

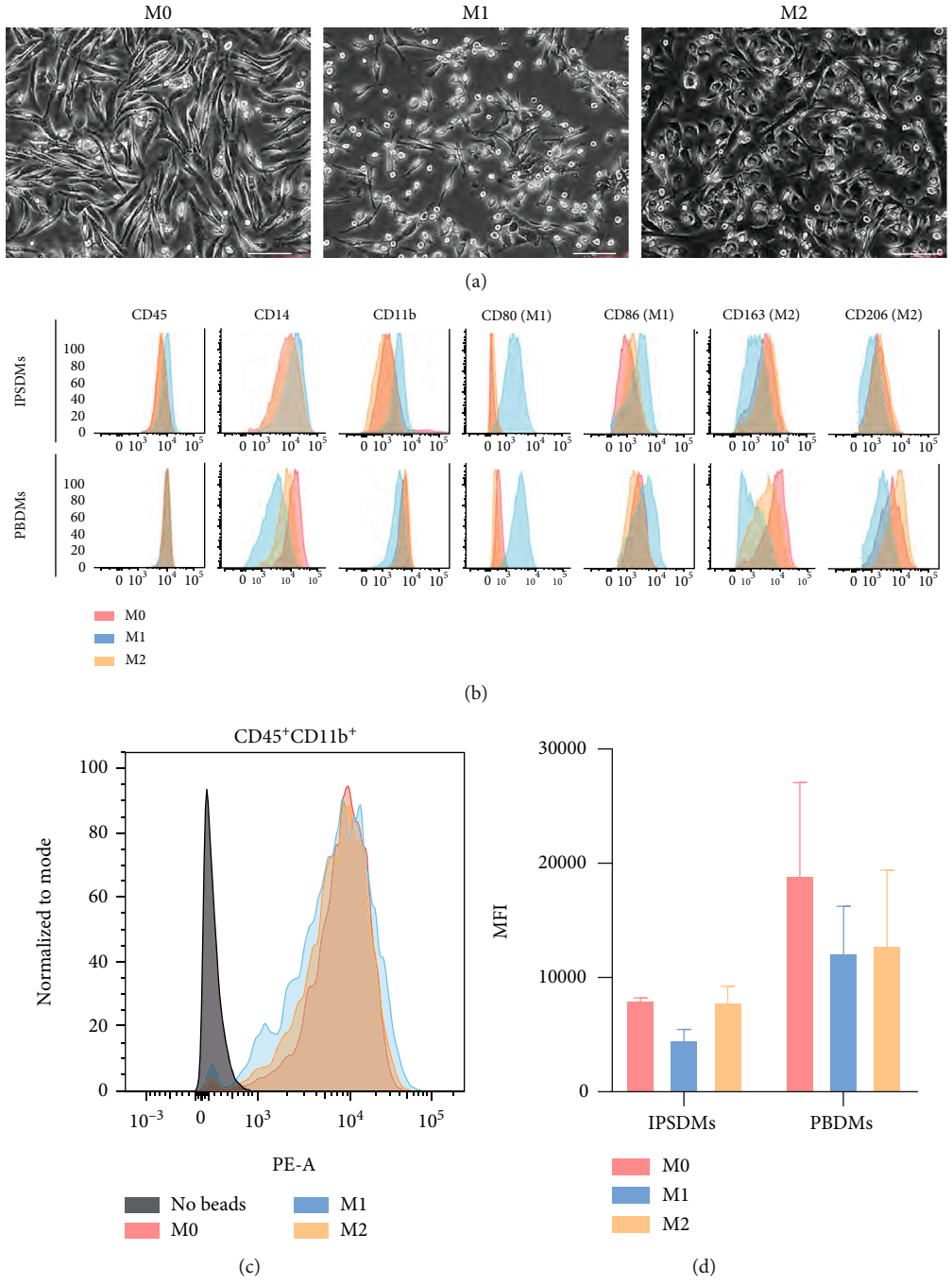

Figure 4: Continued.

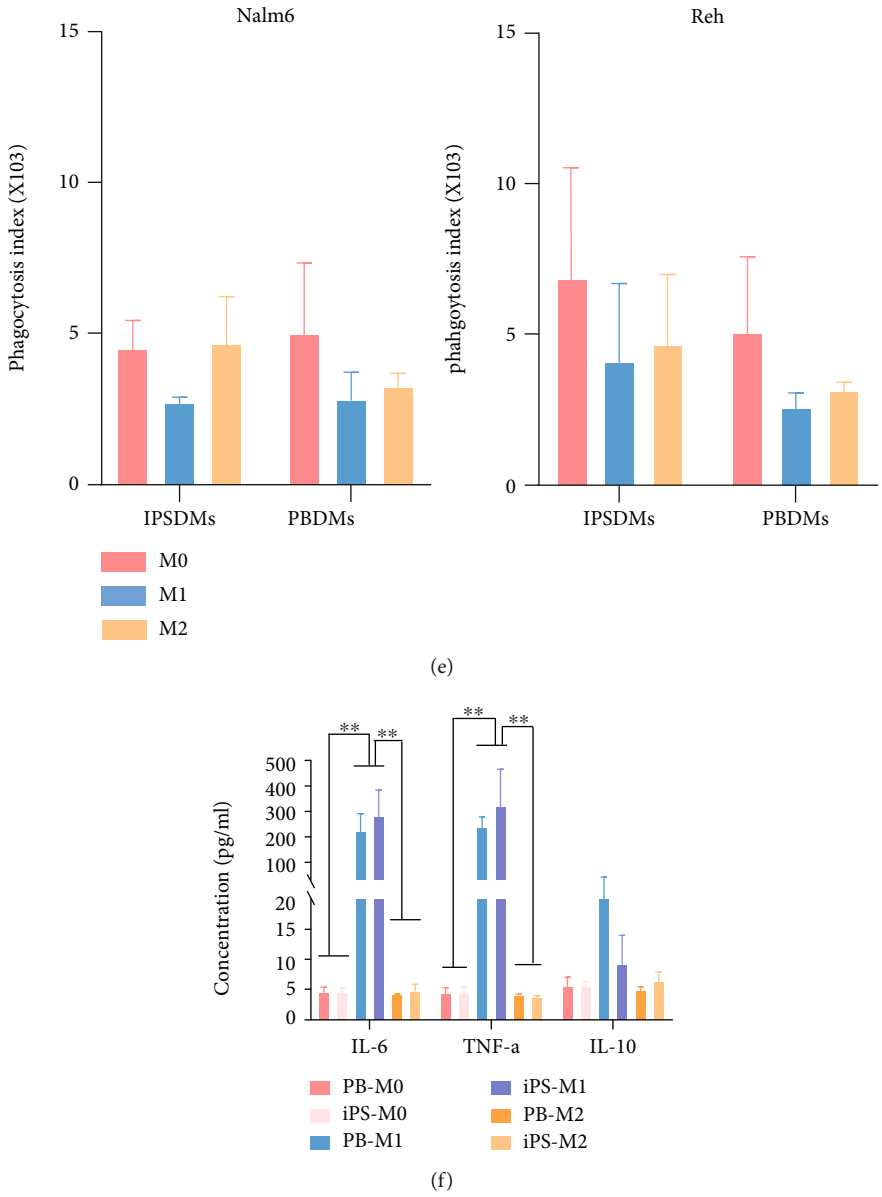

Figure 4: Identification of the different polarized subtypes from IPSDM. (a) Representative bright-filed images of M0 (left panel), M1 (middle panel), and M2 cells (right panel) from hiPSCs. Scale bars, 100 μm. (b) Flow cytometric analysis of markers CD45, CD14, CD11b, CD80 (M1), CD86 (M1), CD163 (M2), and CD206 (M2) of IPSDMs and PBDMs. (c, d) Flow cytometric analysis of the uptake of fluorescent beads by subtypes of IPSDMs and PBDMs. All experiments were performed three times. Error bars, SD. (e) Flow cytometric analysis of phagocytosis of IPSDM and PBDM subtypes on Nalm6 (labeled with Hoechst 33342) and Reh (labeled with Hoechst 33342) (IPSDMs : tumor cells = 1 : 4). Phagocytosis index: the percentage of $V450^+$ macrophages multiplied by the MFI of V450. Error bars, SD. (f) Concentration of IL-6, IL-10, and TNF-α in the supernatants of M0, M1, and M2 cells after 48-hour polarization. $^{**}P < 0.01$.

topic in cancer research due to its close relationship with tumors, and autologous macrophages have been used in clinical trials for cancer treatment in the last century [34]. Recently, CAR-macrophages have been shown to induce a proinflammatory tumor microenvironment and boost antitumor T cell activity in humanized mouse models [3, 35]. Thus, our protocol will facilitate the research and subsequent clinical application of IPSDMs.

In this study, we adjusted the size of EB by increasing the seeding number of iPSCs and produced mature macrophages in a relatively short time with a higher yield. Our final yield of macrophages was close to 50-fold of starting iPSCs, about $\sim 2 \times 10^7$ macrophages per 96-well plate in a month. Compared to the method of van Wilgenburg et al. [21], the yield of macrophages in our protocol was increased by 10-fold in the first month of differentiation (Table S1). According to the seeding iPSCs, the amplification efficiency of our protocol was higher than that of most protocols by one month (Table S1). Recently, Gutbier et al. modified the protocol of van Wilgenburg et al. [21], and the calculated

yield per iPSC (by one month) was comparable to that of our protocol (Table S1) [36]. Di Cui et al. developed a high-yield monolayer differentiation protocol for about 2×10^4 monocytes per seeded hiPSC [30]. The significantly larger scale in cell production and efficient cryopreservation partially compensated for the other limitations of monolayer cultivation. For our research, how to further expand the cumulative yield and extend duration will be the focus. Considering the diversity of various protocols, including PSC lines, culture conditions, differentiation time, and cost performance, the future direction might be to identify the cost-effective, standardized protocols for large-scale clinical application.

Here, we revealed that hematopoietic differentiation originated from the outside of EB and matured inward gradually. The initial size of EB determined the differentiation efficiency but did not affect the phagocytosis of macrophages. Although the most widely known theory is that macrophages derived from circulating monocyte originate in the bone marrow, studies in recent years have shown that some tissue-resident macrophages arise during early embryonic development, independently maintained in a steady state [37–40]. EB is structurally similar to the early stages of embryonic development, which can simulate the original hematopoietic process from extraembryonic structure yolk sac in mammals.

Although our IPSDMs did not show an obvious antitumor effect in vivo, the function of IPSDMs in our protocol was comparable to that of PBDMs. Like PBDMs, our IPSDM treatment caused dissolution and cavities inside the tumor tissues. Compared to IPSDMs, Zhang et al. found that iPSC-derived, CAR-expressing macrophage cell- (CAR-iMac-) treated animals showed reduced ovarian tumor burden [18]. Klichinsky et al. also demonstrated that CAR-M-treated mice demonstrated a marked reduction in SKOV3 tumor burden [35]. Moreover, although all animals eventually progressed, a single infusion of CAR-Ms led to a prolongation of overall survival [35]. Thus, these demonstrate that IPSDMs in combination with CARs will exert its unique effects in clinical solid tumor treatment.

5. Conclusion

In summary, we describe an optimized and reproducible differentiation method to produce mature macrophages from iPSCs in a relatively short time with a higher yield, which may promote cell therapy of macrophages.

Data Availability

Please contact author for data requests.

Ethical Approval

The study was conducted according to the Ethical Principles of Measures for Ethical Review of Biomedical Research Involving Human Beings and the Declaration of Helsinki. The ethics committee of the Children's Medical Center affiliated with Shanghai Jiao Tong University approved the induction experiment for iPS cells (SCMCIRB-K2014050).

Consent

The subject has provided written informed consent for publication of their information in images, videos, etc.

Conflicts of Interest

The authors declare that they have no competing interests.

Authors' Contributions

Y. Li and HF were responsible for conceptualization; SL, ZZ, LS, YZ, YY, LY, HZ, WH, and WW were responsible for investigation; SL, HF, and Y. Li were responsible for analysis; SL, HF, and Y. Li were responsible for writing/reviewing and editing; Y. Li and HF were responsible for funding acquisition.

Acknowledgments

This work was supported in part by the National Key R&D Program of China (2018YFC1313000/2018YFC1313005 to Y. L), National Natural Science Foundation of China (81972341 and 81772663 to Y. Li; 82072896 and 81874078 to H. F, 81900158 to L. S; 81800118 to H. Z), Pudong New Area Science & Technology Development Fund (PKJ2018-Y47), Local High Level University Construction Project of Shanghai Jiao Tong University School of Medicine to Y. Li, Shanghai Municipal Science and Technology Commission (19JC1413500), Shanghai Municipal Education Commission-Gaofeng Clinical Medicine Grant Support (20161310), and Program of Shanghai Academic/Technology Research Leader (21XD1403100) to HF.

Supplementary Materials

Figure S1: flow cytometric analysis of cells on day 14, day 22, and day 30. (a) The percentages of different markers ($CD34^{+-}$ $CD45^+$, $CD45^+CD14^+$, and $CD45^+CD11b^+$) of P3500 protocol (upper panel) and P8000 protocol (lower panel) on day 14. (b) The percentages of different markers ($CD45^+CD14^+$ and $CD45^+CD11b^+$) of P3500 protocol (upper panel) and P8000 protocol (lower panel) on day 22. (c) The percentages of different markers ($CD45^+CD14^+$ and $CD45^+CD11b^+$) of P3500 protocol (upper panel) and P8000 protocol (lower panel) on day 30. Figure S2: validation of the antitumor effect of macrophages in vivo. (a) A line chart of tumor volume over time and (b) the weight of tumors after the mice were sacrificed. (c) Hematoxylin-eosin staining of paraffin sections of tumor tissues. Arrows: macrophages. Scale bars, 250 μm in the left column, 50 μm in the middle and right column. Table S1: summary of protocols for differentiation of macrophages from iPSCs. A list of main publications for macrophage differentiation protocols including coculture with OP9 cells, EB-based protocols, and monolayer cultivation (tissue macrophage subsets such as microglia are not included). Movie: the phagocytosis of IPSDMs toward Reh-Hoechst 33342 was clearly observed in real-time fluorescence imaging of living cells (https://drive.google.com/file/d/1rLwt6xMU46n2u4J5JIOOqWWyHEeGCf7D/view?usp=sharing). *(Supplementary Materials)*

References

[1] W. A. Lim and C. H. June, "The principles of engineering immune cells to treat cancer," *Cell*, vol. 168, no. 4, pp. 724–740, 2017.

[2] T. A. Wynn, A. Chawla, and J. W. Pollard, "Macrophage biology in development, homeostasis and disease," *Nature*, vol. 496, no. 7446, pp. 445–455, 2013.

[3] Y. Chen, Z. Yu, X. Tan et al., "CAR-macrophage: a new immunotherapy candidate against solid tumors," *Biomedicine & Pharmacotherapy*, vol. 139, article 111605, 2021.

[4] S. Lee, S. Kivimäe, A. Dolor, and F. C. Szoka, "Macrophage-based cell therapies: the long and winding road," *Journal of Controlled Release*, vol. 240, pp. 527–540, 2016.

[5] C. Z. W. Lee, T. Kozaki, and F. Ginhoux, "Studying tissue macrophages in vitro: are iPSC-derived cells the answer?," *Nature Reviews. Immunology*, vol. 18, no. 11, pp. 716–725, 2018.

[6] F. Teque, L. Ye, F. Xie et al., "Genetically-edited induced pluripotent stem cells derived from HIV-1-infected patients on therapy can give rise to immune cells resistant to HIV-1 infection," *AIDS*, vol. 34, no. 8, pp. 1141–1149, 2020.

[7] X. Xian, R. Moraghebi, H. Löfvall et al., "Generation of gene-corrected functional osteoclasts from osteopetrotic induced pluripotent stem cells," *Stem Cell Research & Therapy*, vol. 11, no. 1, p. 179, 2020.

[8] D. Hoffmann, J. Sens, S. Brennig et al., "Genetic correction of IL-10RB deficiency reconstitutes anti-inflammatory regulation in iPSC-derived macrophages," *Journal of Personalized Medicine*, vol. 11, no. 3, p. 221, 2021.

[9] E. Navarro-Guerrero, C. Tay, J. P. Whalley et al., "Genome-wide CRISPR/Cas9-knockout in human induced pluripotent stem cell (iPSC)-derived macrophages," *Scientific Reports*, vol. 11, no. 1, p. 4245, 2021.

[10] J. Brault, E. Goutagny, N. Telugu et al., "Optimized generation of functional neutrophils and macrophages from patient-specific induced pluripotent stem cells: ex vivo models of X(0)-linked, AR22(0)- and AR47(0)- chronic granulomatous diseases," *Biores Open Access*, vol. 3, no. 6, pp. 311–326, 2014.

[11] C. Happle, N. Lachmann, M. Ackermann et al., "Pulmonary transplantation of human induced pluripotent stem cell-derived macrophages ameliorates pulmonary alveolar proteinosis," *American Journal of Respiratory and Critical Care Medicine*, vol. 198, no. 3, pp. 350–360, 2018.

[12] K. Haake, A. L. Neehus, T. Buchegger et al., "Patient iPSC-derived macrophages to study inborn errors of the IFN-γ responsive pathway," *Cell*, vol. 9, no. 2, p. 483, 2020.

[13] S. Mukhopadhyay, E. Heinz, I. Porreca et al., "Loss of IL-10 signaling in macrophages limits bacterial killing driven by prostaglandin E2," *The Journal of Experimental Medicine*, vol. 217, no. 2, article e20180649, 2020.

[14] W. Zhao, D. R. Beers, J. R. Thonhoff et al., "Immunosuppressive functions of M2 macrophages derived from iPSCs of patients with ALS and healthy controls," *iScience*, vol. 23, no. 6, article 101192, 2020.

[15] C. Munn, S. Burton, S. Dickerson, K. Bakshy, A. Strouse, and D. Rajesh, "Generation of cryopreserved macrophages from normal and genetically engineered human pluripotent stem cells for disease modelling," *PLoS One*, vol. 16, no. 4, article e0250107, 2021.

[16] D. Hong, J. Ding, O. Li et al., "Human-induced pluripotent stem cell-derived macrophages and their immunological function in response to tuberculosis infection," *Stem Cell Research & Therapy*, vol. 9, no. 1, p. 49, 2018.

[17] E. M. Bernard, A. Fearns, C. Bussi et al., "M. tuberculosis infection of human iPSDM reveals complex membrane dynamics during xenophagy evasion," *Journal of Cell Science*, vol. 134, no. 5, article jcs252973, 2020.

[18] L. Zhang, L. Tian, X. Dai et al., "Pluripotent stem cell-derived CAR-macrophage cells with antigen-dependent anti-cancer cell functions," *Journal of Hematology & Oncology*, vol. 13, no. 1, p. 153, 2020.

[19] S. Senju, M. Haruta, K. Matsumura et al., "Generation of dendritic cells and macrophages from human induced pluripotent stem cells aiming at cell therapy," *Gene Therapy*, vol. 18, no. 9, pp. 874–883, 2011.

[20] A. Kambal, G. Mitchell, W. Cary et al., "Generation of HIV-1 resistant and functional macrophages from hematopoietic stem cell-derived induced pluripotent stem cells," *Molecular Therapy*, vol. 19, no. 3, pp. 584–593, 2011.

[21] B. Wilgenburg, C. Browne, J. Vowles, and S. A. Cowley, "Efficient, long term production of monocyte-derived macrophages from human pluripotent stem cells under partly-defined and fully-defined conditions," *PLoS One*, vol. 8, no. 8, article e71098, 2013.

[22] N. Lachmann, M. Ackermann, E. Frenzel et al., "Large-scale hematopoietic differentiation of human induced pluripotent stem cells provides granulocytes or macrophages for cell replacement therapies," *Stem Cell Reports*, vol. 4, no. 2, pp. 282–296, 2015.

[23] M. Ackermann, H. Kempf, M. Hetzel et al., "Bioreactor-based mass production of human iPSC-derived macrophages enables immunotherapies against bacterial airway infections," *Nature Communications*, vol. 9, no. 1, p. 5088, 2018.

[24] C. Mukherjee, C. Hale, and S. Mukhopadhyay, "A simple multistep protocol for differentiating human induced pluripotent stem cells into functional macrophages," *Methods in Molecular Biology*, vol. 1784, pp. 13–28, 2018.

[25] M. Lopez-Yrigoyen, A. May, T. Ventura et al., "Production and characterization of human macrophages from pluripotent stem cells," *Journal of Visualized Experiments*, vol. 158, no. 158, 2020.

[26] S. Monkley, J. K. Krishnaswamy, M. Göransson et al., "Optimised generation of iPSC-derived macrophages and dendritic cells that are functionally and transcriptionally similar to their primary counterparts," *PLoS One*, vol. 15, no. 12, article e0243807, 2020.

[27] M. D. Yanagimachi, A. Niwa, T. Tanaka et al., "Robust and highly-efficient differentiation of functional monocytic cells from human pluripotent stem cells under serum- and feeder cell-free conditions," *PLoS One*, vol. 8, no. 4, article e59243, 2013.

[28] K. Takata, T. Kozaki, C. Z. W. Lee et al., "Induced-pluripotent-stem-cell-derived primitive macrophages provide a platform for modeling tissue-resident macrophage differentiation and function," *Immunity*, vol. 47, no. 1, pp. 183–198.e6, 2017.

[29] X. Cao, G. K. Yakala, F. E. van den Hil, A. Cochrane, C. L. Mummery, and V. V. Orlova, "Differentiation and functional comparison of monocytes and macrophages from hiPSCs with peripheral blood derivatives," *Stem Cell Reports*, vol. 12, no. 6, pp. 1282–1297, 2019.

[30] D. Cui, A. Franz, S. A. Fillon et al., "High-yield human induced pluripotent stem cell-derived monocytes and macrophages are functionally comparable with primary cells," *Frontiers in Cell and Development Biology*, vol. 9, article 656867, 2021.

[31] H. Zhang, C. Xue, R. Shah et al., "Functional analysis and transcriptomic profiling of iPSC-derived macrophages and their application in modeling Mendelian disease," *Circulation Research*, vol. 117, no. 1, pp. 17–28, 2015.

[32] J. Shi, C. Xue, W. Liu, and H. Zhang, "Differentiation of human-induced pluripotent stem cells to macrophages for disease modeling and functional genomics," *Current Protocols in Stem Cell Biology*, vol. 48, no. 1, article e74, 2019.

[33] K. Biswas Subhra and A. Mantovani, "Orchestration of metabolism by macrophages," *Cell Metabolism*, vol. 15, no. 4, pp. 432–437, 2012.

[34] N. R. Anderson, N. G. Minutolo, S. Gill, and M. Klichinsky, "Macrophage-based approaches for cancer immunotherapy," *Cancer Research*, vol. 81, no. 5, pp. 1201–1208, 2021.

[35] M. Klichinsky, M. Ruella, O. Shestova et al., "Human chimeric antigen receptor macrophages for cancer immunotherapy," *Nature Biotechnology*, vol. 38, no. 8, pp. 947–953, 2020.

[36] S. Gutbier, F. Wanke, N. Dahm et al., "Large-scale production of human iPSC-derived macrophages for drug screening," *International Journal of Molecular Sciences*, vol. 21, no. 13, p. 4808, 2020.

[37] F. Ginhoux, M. Greter, M. Leboeuf et al., "Fate mapping analysis reveals that adult microglia derive from primitive macrophages," *Science*, vol. 330, no. 6005, pp. 841–845, 2010.

[38] G. Hoeffel, Y. Wang, M. Greter et al., "Adult Langerhans cells derive predominantly from embryonic fetal liver monocytes with a minor contribution of yolk sac-derived macrophages," *The Journal of Experimental Medicine*, vol. 209, no. 6, pp. 1167–1181, 2012.

[39] C. Schulz, E. G. Perdiguero, L. Chorro et al., "A lineage of myeloid cells independent of Myb and hematopoietic stem cells," *Science*, vol. 336, no. 6077, pp. 86–90, 2012.

[40] D. Hashimoto, A. Chow, C. Noizat et al., "Tissue-resident macrophages self-maintain locally throughout adult life with minimal contribution from circulating monocytes," *Immunity*, vol. 38, no. 4, pp. 792–804, 2013.